Global investigation of the influence of the phase of subharmonic excitation of a driven system

Didier Dangoisse, Jean-Christophe Celet, and Pierre Glorieux
Laboratoire de Spectroscopie Hertzienne, associé au CNRS, Centre d'Etudes et Recherches Lasers et Applications, Université des Sciences et Technologies de Lille, F-59655 Villeneuve d'Ascq Cédex, France
(Received 29 January 1997)

Adding a small subharmonic perturbation to the driving signal of a modulated laser allows one to control its dynamics. The influence of the phase of such a perturbation has been investigated both experimentally and by numerical simulations on a model of a fiber laser subjected to pump modulation. Depending on the operating conditions, the laser destabilizes through a period-doubling cascade or via quasiperiodicity. Suitably phased subharmonic perturbations can stabilize periodic orbits, shift the whole bifurcation diagram, and induce new crises. Experimental observations are in excellent agreement with the predictions from a simple model of the fiber laser. [S1063-651X(97)09607-4]

PACS number(s): 05.45.+b

I. INTRODUCTION

Dynamics of nonlinear systems may be strongly affected by a small perturbation of some control parameter. This effect depends strongly on the characteristics of the perturbation and on the dynamical regime of the system under consideration. For instance, the system is expected to be extremely sensitive to any perturbation in the vicinity of a bifurcation point. Moreover, since Ott, Grebogi, and Yorke proposed an algorithm to keep a chaotic system on one of the unstable periodic orbits that are embedded inside a chaotic attractor, there has been a great deal of interest in the control of chaos [1]. Basically, weak feedback using information on the dynamical state of the system allows one to control and to lock it in an unstable periodic orbit. This idea triggered a lot of experiments and variants in all the domains of application of nonlinear dynamics, e.g., chemical reactions, magnetoelastic ribbons, lasers, etc. These methods comprise the feedback techniques that control nonlinear dynamics. Nonfeedback techniques in which some parameter is externally driven, often by an externally applied sinusoidal signal, have also recently received renewed interest. They are known to induce spectacular effects. In particular, it has been observed that a small modulation may suppress or induce chaos [2–6].

A nonfeedback control method can be modeled in a system driven by a sinusoidal modulation $r_1\cos\Omega\tau$ as

$$\frac{d\vec{x}}{d\tau}=\vec{F}(\vec{x},r_1\cos\Omega\tau,r_2\cos(\Omega'\tau+\varphi)).$$

Recently there has been some interest in the influence of the phase φ of the secondary modulation $r_2\cos(\Omega'\tau+\varphi)$. This is relevant only in problems where Ω and Ω' are commensurate. The influence of the phase of a subharmonic perturbation, such as $\Omega/\Omega'=n$ of a modulated system, has already been extensively explored in the vicinity of period-doubling bifurcations by Pisarchik and co-workers on a CO_2 laser with modulated losses. They essentially studied the phase dependence of small signal (de)amplification near T-$2T$ and $2T$-$4T$ bifurcations [7,8]. Meucci *et al.* also showed that the phase of the parametric perturbation is a crucial parameter that plays an important role in determining the resultant dynamics of the system [9]. Yang, Qu, and Hu recently studied numerically the phase effect of a second periodic forcing in the Duffing equation [10]. A bifurcation analysis of two-tone modulation of the fiber laser has recently been done by Newell *et al.* [11]. They concentrated on the analysis of a second subharmonic modulation in the vicinity of the T-$2T$ bifurcation and have been able to derive analytical expressions for the laser response in these conditions. Closely related works concern the influence of a very small detuning between the main modulation and the subharmonic one, i.e., $|\Omega/n-\Omega'|\ll\Omega$, since such a detuning may be regarded as a small drifting phase [12,13]. Let us emphasize that the amplitude of this second perturbation is always much—typically 40 times—smaller than the main (driving) perturbation which places the system in a highly nonlinear domain.

Most of the previous works on the effect of a second perturbation considered a *local* point of view in the parameter space, i.e., fixed values of the parameters. Here the influence of the phase is more *globally* investigated, i.e., we have studied the effects for second and fourth subharmonic modulations in a driven system by measuring changes in full bifurcation diagrams. Specifically, our experiments and numerical simulations concentrate on two kinds of transitions to chaos, namely, when the system evolves to chaos either through a cascade of period-doubling bifurcations or through quasiperiodicity. The experiments have been made on a Nd^{3+}-doped fiber laser because it displays the two abovementioned scenarios of transition to chaos and because it can be simulated numerically using a simple model. Although the additional subharmonic modulation is small, we have found that it may lead to significant changes in the whole bifurcation diagram. We have observed that periodic states may disappear or emerge as a result of the second modulation. All previous experimental and numerical studies concentrated on specific bifurcation points and have led to interesting scaling laws. However, they do not indicate how states disappear or emerge as the result of these small amplitude modulations. The main objective of this paper is to investigate these global changes for a periodically modulated laser.

This paper is organized in the following way: in the next section we recall the characteristics of the doped fiber laser and of its model used throughout this paper. The third sec-

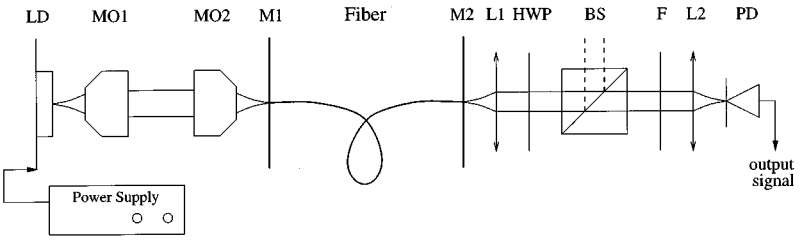

FIG. 1. Schematic view of the experimental setup. LD, laser diode; MO, microscope objective; M, mirror; L, lens; HWP, half-wave plate; BS, beam splitter; F, filter; PD, photodiode.

tion reports on the phase dependence of the changes induced by the parametric modulation on the period-doubling cascade transition to chaos and the associated chaotic regimes. These predictions are compared in the fourth section with experimental observations of the fiber laser operated in the corresponding situations. The case of a transition via quasiperiodicity is investigated both numerically and experimentally in the two following sections. Conclusions and discussion are presented in the last section.

II. THE FIBER LASER

The doped fiber laser has been chosen to study the phase effects of a small parametric perturbation for both technical and physical reasons. The main reason is its versatility, i.e., its ability to be operated in a variety of dynamical regimes. By using various modulation conditions, it has been possible to induce both period-doubling cascades and quasiperiodicity in this system. Moreover, the fiber laser exhibits relaxation oscillations in the 10-kHz range, allowing easy modulation and detailed observation of its dynamics. The characteristics of the laser and its model were discussed in detail in [14]. In this section, we recall the parameters of the model and of the experimental setup which are of interest in the following sections.

A schematic view of the experiment is given in Fig. 1. The key element is the fiber laser, which is essentially made of a 3.5-m-long Nd^{3+} doped fiber placed between mirrors with reflection coefficients of 95 and 99.5 % at the operating wavelength of 1.06 μm. Therefore, the lifetime of the photons inside the cavity τ_c which scales times in the model is equal to 1.67×10^{-7} s and the lifetime of population inversion is approximately equal to 250 μs, leading to a value of the reduced relaxation rate for population inversion γ of 0.67×10^{-3}. With these values of the parameters, the standard relaxation oscillation frequency of the laser is 24.7 $\sqrt{A-1}$ kHz [15]. In typical conditions, A is approximately equal to 2 and the main driving is achieved at around 10 kHz, i.e., at about half the relaxation oscillation frequency (see Table I). Pump modulation is achieved by acting on the current injected in the pump diode. This current is driven by two frequency synthesizers phase-locked to one another and delivering two signals with harmonic frequencies and a controlled phase difference. In this study we consider only qualitative behaviors, e.g., shifts of bifurcation points and changes in dynamical regimes; therefore, only the total intensity or one polarization component needs to be monitored in the experiments. Periodic sampling of the fiber laser intensity at the driving modulation has been used throughout this work, except in some rare situations. This technique allows clear display and direct observation and identification of the bifurcation diagrams of the laser on an oscilloscope. For fixed values of the parameters, return maps have also been used. Such maps are experimentally obtained through the technique of cascade sampling already used in our previous experiments [14]. They proved useful in assigning quickly quasiperiodic regimes discussed in Secs. IV and V. In most experiments and simulations reported here, we have chosen the pump parameter A as a control parameter. Several other choices are possible. We have checked that qualitatively similar results are obtained when the driving amplitude r_1 or the driving frequency Ω is chosen instead of A as the swept parameter.

As the laser emits radiation linearly polarized in two directions, it has been modelized as a two-mode system, each mode being associated with one polarization eigenstate of the laser. The corresponding model is an extension of the so-called class-B model in which a term has been added to take care of the high level of spontaneous emission in this laser and the mode-coupling parameter β has been introduced to account for competition of the two laser subsystems. The dynamical variables are the population inversion and the intensity in each polarization state. The model is written as [14]

$$\dot{m}_i=(d_i+\beta d_j-1)m_i+a(d_i+\beta d_j),$$

$$\dot{d}_1=\gamma[A(\tau)/(1+\beta)-(1+m_1+\beta m_2)d_1],$$

$$\dot{d}_2=\gamma[\alpha A(\tau)/(1+\beta)-(1+m_2+\beta m_1)d_2],$$

where $i=1$ and 2, $j=3-i$, and m_i and d_i are the reduced intensities and population inversions of the subsystems associated with each polarization mode. The dots represent the derivatives with respect to a reduced time $\tau=t/\tau_c$. γ is the reduced relaxation time of population inversion in units of τ_c. a is a parameter characterizing spontaneous emission, α is a measure of the relative efficiency of the pumping in the two sublasers, and β is a cross-saturation coefficient. $A(\tau)$ is the pump parameter common to the two laser sub-

TABLE I. Parameters used in the numerical simulations.

Parameters	T-doubling	Quasiperiodicity
β	0.43	0.43
α	0.86	0.84
A	1.75–2	3.65
γ	$0.67\ 10^{-3}$	$0.67\ 10^{-3}$
a	$1.8\ 10^{-4}$	$1.2\ 10^{-4}$
Ω/Ω_R	0.58–0.48	0.4
r_1	0.42	0.75–0.79
r_2	0.01	0.02

systems. In our experiments the laser is driven by acting on this parameter, which is easily achieved by modulating the current injected in the pump laser diode. In the presence of the main and subharmonic modulations, the parameter $A(\tau)$ can be written as

$$A(\tau)=A[1+r_1\cos\Omega\tau+r_2\cos(\Omega\tau/n+\varphi)],$$

where A is the pump parameter in the absence of modulation, r_1 and Ω are the amplitude and frequency, respectively, of the main modulation, r_2 is the amplitude of the perturbation, φ its phase, and n is the rank of the subharmonic. Here, two subharmonic frequencies are used, corresponding to $n=2$ or 4.

All simulations reported below have been obtained with the model given above and taking as initial conditions the results obtained with the preceding value of the control parameter, namely, A in Secs. III and IV and r_1 in Secs. V and VI and always with increasing values unless otherwise specified. This procedure is important when the objective is a comparison with the experiments because, due to the presence of boundary crises, there may exist large domains of generalized multistability, i.e., domains of coexistence between several attractors. In the first series of simulations discussed in the next section, we will present bifurcation diagrams obtained with both increasing and decreasing A to exhibit clearly the effects due to the existence of such hysteresis phenomena. Operating parameters of the laser were chosen so that it evolves toward chaos through either a period-doubling cascade or through quasiperiodicity both in experiments and in the numerical simulations. A key parameter of these experiments is the ratio of the modulation frequency Ω to the relaxation oscillation frequency Ω_R of the laser (both in units of τ_c^{-1}). In accordance with previous results, the transition to chaos through a period-doubling cascade is readily obtained as $\Omega/\Omega_R\approx 0.5$ if other parameters are adequately chosen, while, if $\Omega/\Omega_R\approx 0.4$, this evolution occurs via quasiperiodicity. Note that in both cases addition of subharmonic modulation automatically implies subharmonic response. This trivial (linear) effect should be distinguished from the nonlinear effects discussed below.

III. PERIOD-DOUBLING CASCADE—SIMULATIONS

The period-doubling cascade is the most frequent scenario of transition to chaos in the fiber laser. Numerical simulations of the driven fiber laser were first carried out on the model presented in the preceding section for a set of parameters corresponding to the experimentally accessible situation and in which the response of the system to pump modulation evolves to chaos through a period-doubling transition as the pump parameter A increases (see Table I and Figs. 2 and 3). The regions of chaotic behavior end with a boundary crisis in which the chaotic attractor is destroyed and at larger A values the system evolves in another attractor, here a periodic attractor which also evolves as A is further increased.

Let us first discuss the different kinds of regimes for the subharmonic modulation, as they come from the observation of the role of the amplitude r_2 of the second modulation as illustrated, for instance, in Fig. 2. Three domains may be distinguished.

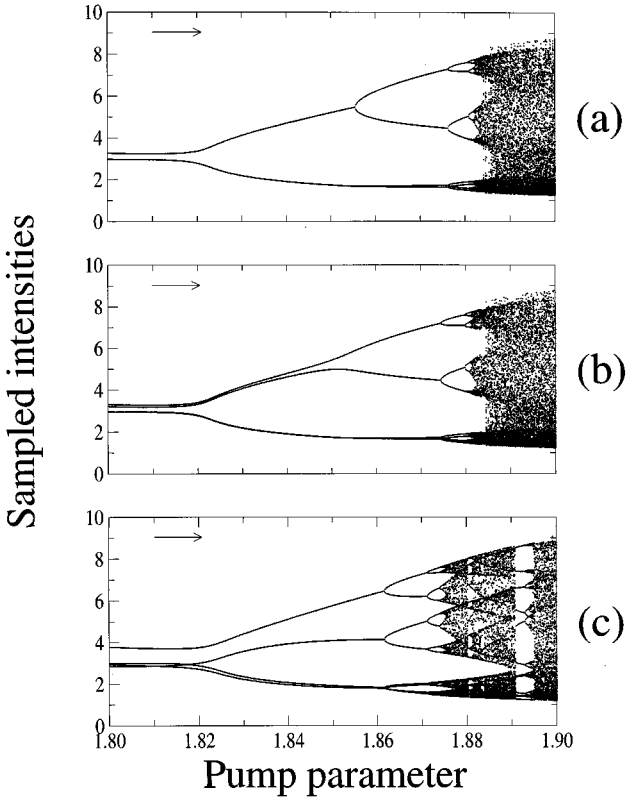

FIG. 2. Influence of the amplitude of the fourth ($n=4$) subharmonic perturbation with $\varphi=0$. (a) No subharmonic modulation $r_2=0$, (b) extremely weak subharmonic modulation $r_2=5\times10^{-4}$, (c) weak subharmonic modulation $r_2=5\times10^{-3}$.

(1) At very small values of r_2, typically $r_2\leqslant 10^{-4}$ with the conditions of Fig. 2, the main effect of the additional modulation is to create a $4T$ periodic response in the low-A region of the bifurcation diagram where the system was T or $2T$ periodic for $r_2=0$. As the $2T$-$4T$ bifurcation is approached, the amplitude of the $4T$ component of the response increases, as evidenced by the splitting of the branches of the $4T$ solution [see region $1.845\leqslant A\leqslant 1.86$ in Figure 2(b)]. This is the amplification of subharmonic perturbations already discussed in [16,17] and corresponds to a zone of linearity with respect to r_2.

(2) For larger modulations, namely, modulations in the range $r_2\sim 10^{-4}$–10^{-2}, the splitting of the $4T$ branch becomes prominent and new effects appear regarding the position and the nature of the other bifurcations. This is the topic of the present paper. In this domain, the system would be linear with respect to r_2 in the absence of r_1.

(3) If r_2 is further increased, typically $r_2\sim 10^{-1}$ and above, this additional modulation may not be considered small with respect to the main one. This is the domain of the dynamics of systems subjected to two equally important modulations and will not be considered here.

Examples of the results commonly obtained with $r_2\ll r_1$ are displayed in Figs. 2 and 3 where we have reported bifurcation diagrams to be derived from the observation of one polarization component with A as a control parameter and, in the case of subharmonic perturbation, with $n=4$. The top diagram of Fig. 3 is a reference in the absence of the second modulation ($r_2=0$) and the two lower ones illustrate the

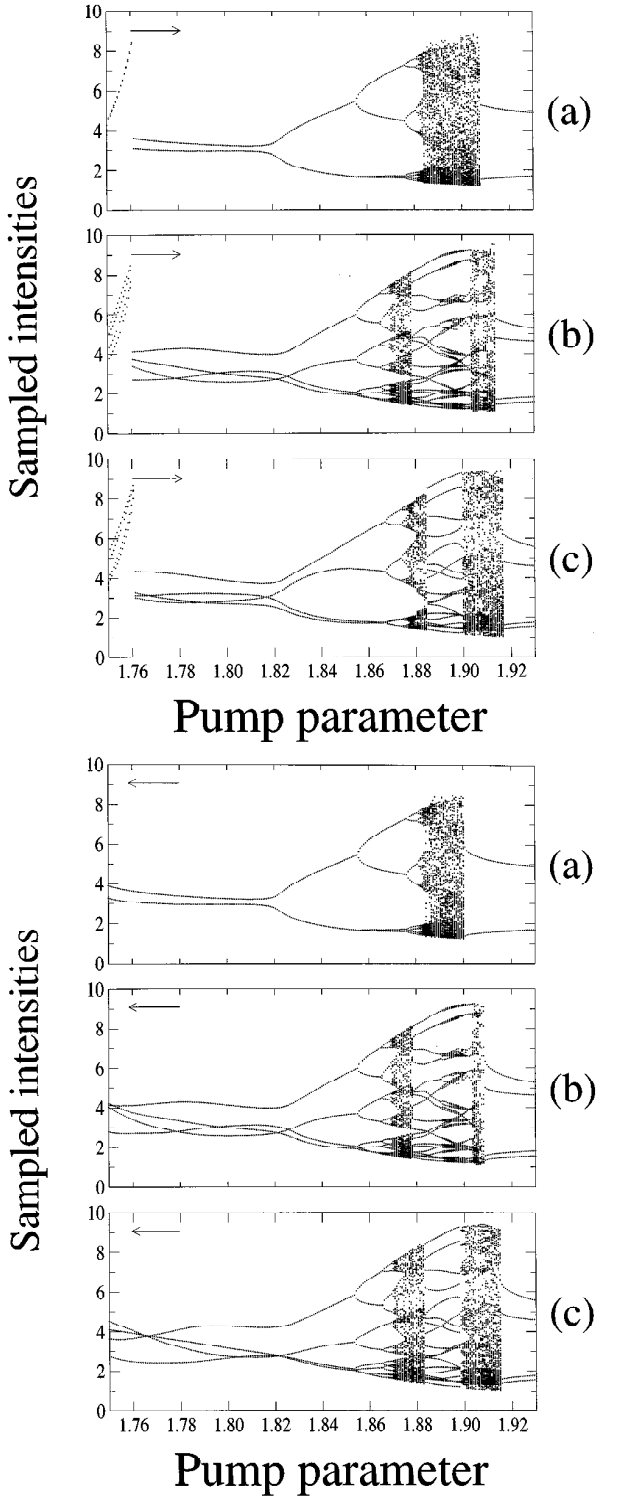

FIG. 3. Cascades of period-doubling bifurcations calculated for the fiber laser model (a) (top) reference diagram in the absence of subharmonic perturbation, (b) in the presence of in phase ($\varphi=0$), and (c) dephased ($\varphi=2\pi/9$) subharmonic ($n=4$) modulation for increasing (right-pointing arrows) and decreasing (left-pointing arrows).

phase dependence of the action of the second (subharmonic) perturbation. These diagrams are obtained for phase shifts $\varphi=0$ and $2\pi/9$. The latter value was chosen since it maximizes many of the phenomena discussed below. The existence of boundary crises, i.e., switching from a chaotic attractor to a new attractor with a different basin of attraction, is accompanied by hysteresis phenomena. To illustrate this, all diagrams are presented in Fig. 3 with both increasing and decreasing values of the control parameter A. Comparison of Figs. 3(b) and 3(c) with the reference one ($r_2=0$) [Fig. 3(a)] shows that, depending on the phase of subharmonic modulation relative to the driving, this perturbation induces effects of different kinds which can be classified as follows.

(i) *Shift and magnification of the whole bifurcation diagram with respect to the reference one*. The scenario of transition to chaos through a period-doubling cascade may be preserved but the bifurcation points are shifted by an amount which is phase dependent. Moreover, the distance between corresponding bifurcations may also be altered by the presence of the second perturbation. An example of such phenomena is displayed in Fig. 3. In the absence of subharmonic perturbation [Fig. 3(a)], the system undergoes a period-doubling cascade transition to chaos for $1.84\leqslant A\leqslant 1.885$ with $4T\rightarrow 8T$ and $8T\rightarrow 16T$ bifurcations at $A=1.8767$ and 1.8812, respectively. When the second modulation is applied, these transitions are shifted to lower A values; the magnitude of this shift depends on both the amplitude and the phase of the subharmonic perturbation. As an example, the $4T\rightarrow 8T$ bifurcation that occurs in the unperturbed system at $A=1.8767$ is shifted to $A=1.8557$ and the $8T\rightarrow 16T$ bifurcation appears at $A=1.8655$ when an in-phase subharmonic bifurcation is applied. For a different phase φ of the subharmonic bifurcation, e.g., $\varphi=2\pi/9$, the shifts are much weaker, since the above-mentioned bifurcations appear at $A=1.8677$ and $A=1.8745$, respectively. More generally, numerical simulations indicate that the magnitude of the effect strongly depends on the phase φ of the subharmonic bifurcation with respect to the main one. The details of this process vary with the operating conditions of the laser and it should also be noted that these shifts are almost always accompanied by dilatation of the period-doubling cascades, as shown in Fig. 3.

(ii) *Generation of periodic regimes in a region where the reference system, i.e., the unperturbed one, is chaotic, and vice-versa*. On one hand, this may be a simple consequence of the shift and magnification effects presented above, as, e.g., in the conditions of Fig. 3; for $A=1.870$ the unperturbed system is $4T$ periodic and the perturbed one is chaotic for $\varphi=0$ and $8T$ periodic for $\varphi=2\pi/9$. On the other hand, this could also be due to a change in the attractor, as, e.g., with the same conditions but in the range around $A=1.885$, where the unperturbed system is chaotic and the perturbed one is $20T$ periodic for $\varphi=0$ and $\varphi=2\pi/9$. Both perturbed periodic regimes correspond to limit cycles with no obvious connection with the original chaotic attractor. Additional studies show that some periodic windows that appeared within the parameter region of chaotic behavior are canceled and new windows may be created. An example of this is obtained slightly outside the range explored in Fig. 3: a new $8T$ periodic regime is created near $A=1.97$ for $\varphi=0$ in a region in which the unperturbed laser is chaotic. Conversely, near $A=2$ the unperturbed system is $9T$ periodic, while it is chaotic in the presence of subharmonic modulation at the two phases used in this set of simulations.

(iii) *Crisis induction and suppression*. A simple examina-

tion of the bifurcation diagrams shows that the second perturbation induces qualitative changes in these diagrams, in particular in the scenario of transition into and out of chaos. Several situations are typically encountered: a period-doubling cascade may be truncated or extended by the second perturbation. The latter effect is observed near $A=1.885$, where the unperturbed system undergoes an internal crisis in which the attractor suddenly expands, as shown in Fig. 3(a). This crisis is postponed by the second modulation for both reference phases. Conversely, boundary and internal crises can be observed in the presence of the subharmonic modulation, while they are absent from the reference bifurcation diagram. For instance, additional simulations demonstrate that a boundary crisis occurs at $\varphi=2\pi/9$ and $A=1.97$, where the chaotic attractor obtained with the main driving only is destroyed in favor of an $8T$ limit cycle for $\varphi=0$ and of another chaotic attractor for $\varphi=2\pi/9$. All these effects are strongly phase dependent but we have not found any simple relation between the dephasing φ and the magnitude of the shift of the bifurcation points. In the system considered here, several attractors may coexist, a situation commonly associated with the existence of boundary crises. When this occurs, the second perturbation usually helps the system to jump into the basin of attraction of the other and the crisis occurs for lower values of the driving parameter. Note that this is a highly nonlinear contribution of the second modulation in spite of its low value and it may be attributed to the extreme sensitivity of the trajectories which explore the limits of the basin of attraction. It is classical that near these limit zones, the ''equivalent potential'' of the system presents extrema, i.e., allows for large explorations with a small change of parameter. Moreover, here this change is parametrically resonant and its phase may be adjusted to enhance the efficiency of the perturbation. Again using this potential analogy, it is clear that the phase of the perturbation should play a major role. Depending on its timing with respect to the laser response, the additional perturbation may push the system towards the boundary limit or pull it from it, therefore enhancing or retarding the switching toward a new attractor basin of attraction.

The above classification is somewhat contrived, but it offers a global view of how the subharmonic modulation alters the dynamics of this nonlinear system. Such a global point of view is necessary in order to understand the action of the subharmonic perturbation. A local point of view would have shown only apparently erratic changes between chaotic, quasiperiodic, and periodic regimes with no overview of the general organization. Locally, these changes can occur in both directions, i.e., they can induce or prevent the appearance of chaos and depending on the parameters chosen almost all changes in dynamical regimes are possible. The general point of view adopted here reveals the organization of these changes and allows one to understand how contradictory effects such as positive and negative shifts may coexist.

Similar simulations were repeated in the case of second subharmonic perturbation, i.e., $n=2$. Corresponding results are given in Fig. 4 for various amplitudes of the modulation. They show that the effects are essentially of the same nature as in the case of fourth subharmonic perturbation, except for three points. (i) Because this is a second subharmonic modulation, there are only two branches far from the nonlinear region and (ii) new possiblities open because of the coexistence of several attractors. For instance, the diagram for $r_2=0.002$ shows that there is a switching from one $2T$ regime to another one, which gives rise to the period-doubling cascade as A is increased. The diagram obtained with $r_2=0.004$ shows that the switching point shifts to higher A values as r_2 is increased and at large r_2 values, typically above $r_2=0.01$, the system switches directly from this $2T$ attractor to the other $2T$ attractor, which is the one that appears beyond the domain of the period-doubling cascade, i.e., with $1.91\leqslant A\leqslant 1.96$. For the parameters used in these simulations and as A varies, the system switches between two or three different $2T$ attractors depending on the value of r_2. As this parameter is varied, the continuous transition between attractors that occurs at low r_2 values is transformed into an abrupt one with associated hysteresis phenomena. (iii) The system is more sensitive to second than to fourth subharmonic modulation, as is usual for such parametric modulations.

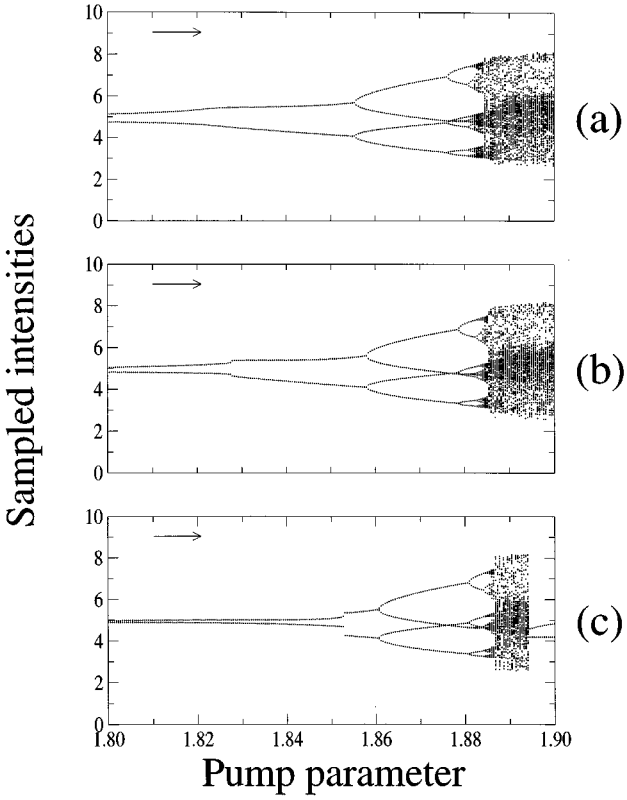

FIG. 4. Same as Fig. 3 with $n=2$ subharmonic modulation. (a) Reference diagram in the absence of subharmonic perturbation, (b) and (c) in the presence of in-phase ($\varphi=0$) subharmonic modulation with amplitude $r_2=2\times10^{-3}$ and $r_2=4\times10^{-3}$, respectively.

IV. PERIOD-DOUBLING CASCADE—EXPERIMENTS

A series of experiments has been carried out in order to check the predictions of the model. We chose to concentrate here on the case $n=4$. The pump power is modulated simultaneously at 7 kHz and 1.75 kHz; the former frequency is approximately equal to half the measured relaxation frequency of the fiber laser. The pump power is chosen to be

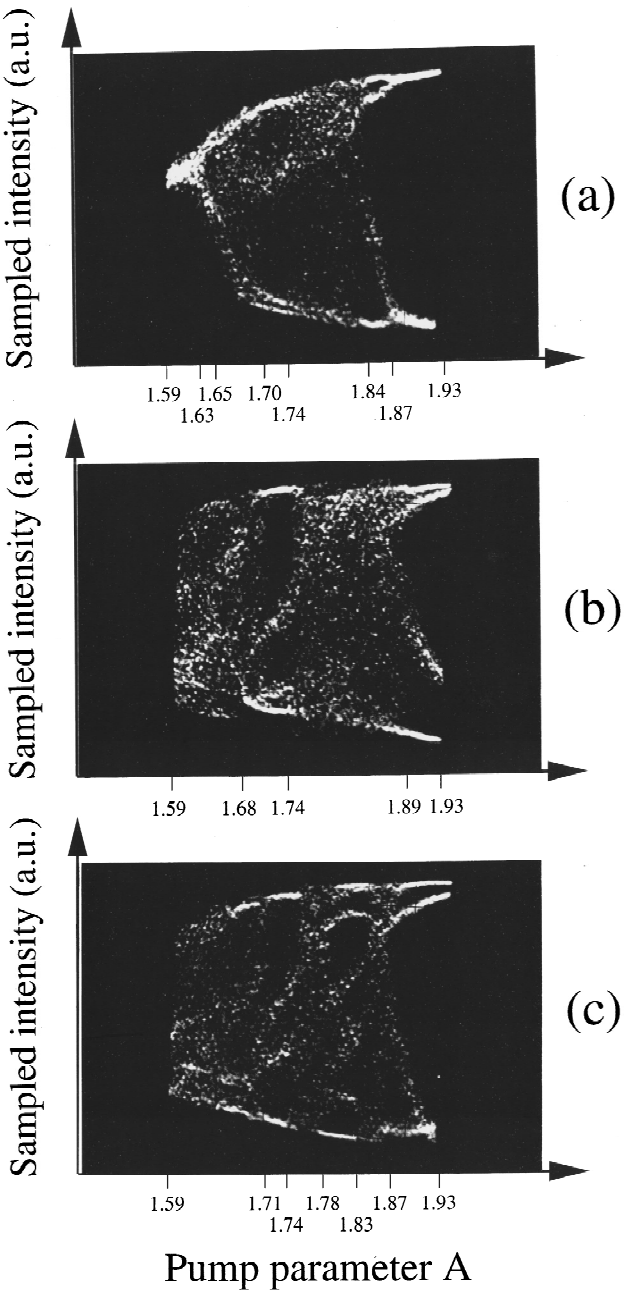

FIG. 5. Experimental bifurcation diagrams in the case of $n=4$ subharmonic perturbation. (a) Reference diagram in the absence of perturbation, (b) in the presence of in-phase ($\varphi=0$), and (c) dephased ($\varphi=2\pi/9$) subharmonic perturbation at the same frequency.

the control parameter for obtaining the bifurcation diagram. Sweeps of the control parameter are such that the range $A=1.59-1.93$ is spanned and typically $r_2=0.025r_1$. Note that when it is applied alone, the second perturbation is much less efficient than the main one because the latter corresponds to the condition of parametric resonance.

Figure 5 shows several bifurcation diagrams obtained under these conditions. Figure 5(a) displays the reference diagram without the subharmonic perturbation, and 5(b) and 5(c) are the corresponding diagrams for different phases ($\varphi=0$ and $\varphi=2\pi/9$) of the subharmonic perturbation. They are in good agreement with the predictions of numerical simulations given in the preceding section.

(i) The shift of the bifurcation points is clear, in agreement with prediction. For instance, on the left-hand sides of the photographs ($A=1.59$), the regime is T periodic in the reference diagram but becomes chaotic when the subharmonic perturbation is applied. Comparison of the right-hand parts of the three diagrams shows that the general shape of the bifurcation diagram is not changed by the subharmonic bifurcation and that the dominant effect is a shift which is larger for $\varphi=0$ than for $\varphi=2\pi/9$, in accordance with the prediction of the numerical simulations of the preceding section.

(ii) Creation of periodic windows in the chaotic domain and vice-versa agrees with prediction. The $4T$ periodic regimes, which are visible, for instance, in the central part ($1.71\leqslant A\leqslant 1.74$ and $1.78\leqslant A\leqslant 1.83$) of Fig. 5(c) are absent from the same region in the reference diagram.

(iii) Induction of crises is consistent with prediction. A small internal crisis is visible on the left-hand side of Fig. 5(b) at $A=1.68$, where the system switches from a chaotic to a $4T$ periodic attractor.

V. QUASIPERIODICITY—SIMULATIONS

When the ratio of the modulation frequency to the relaxation frequency is changed from 0.5 to 0.4, the transition to chaos occurs at larger A values and through quasiperiodicity instead of the cascade of period-doubling bifurcations. Then as the pump modulation is increased, the laser first responds at the modulation frequency, and at larger modulation amplitudes a new frequency with no simple arithmetic relation to the driving one appears in the laser output intensity. This transition may be reproduced in the fiber laser model presented above for the set of parameters given in Table I. Note also that the spontaneous-emission coefficient a has to be changed significantly in order to reach quasiperiodicity in the range of parameters corresponding to experiment. Quasiperiodicity could also be obtained for different parameters but we just want to investigate with a plausible model the effect of a weak subharmonic parametric perturbation in the transition via quasiperiodicity. The Poincaré section of the attractor given by taking periodic samples, i.e., stroboscoping at the modulation frequency, clearly exhibits a transition at $r_1=0.776$ in Fig. 6. A Fourier transform of the laser response to modulation shows that the new frequency that appears at the bifurcation is approximately equal to 0.27Ω. In presence of the weak subharmonic perturbation, we note different effects in addition to the trivial linear effect. They are (i) the shift of the bifurcation to quasiperiodic response towards higher modulation values, and (ii) an enlargement and a shift of the periodic windows.

For specific ranges of parameters, it is possible to control the dynamics of the laser by acting only on the phase of the second modulation. For instance, it is possible to switch from a quasiperiodic regime to a periodic one by taking advantage of the shift (i), e.g., by driving the system with an amplitude of $r_1=0.777$ and applying a small subharmonic modulation with $r_2=0.02$ and $\varphi=0$ [see Figs. 6(a) and 6(b)]. Similarly, a periodic regime associated with a window inside a chaotic domain can be transformed into a quasiperiodic one by using the shift (ii) of this window induced by the subharmonic

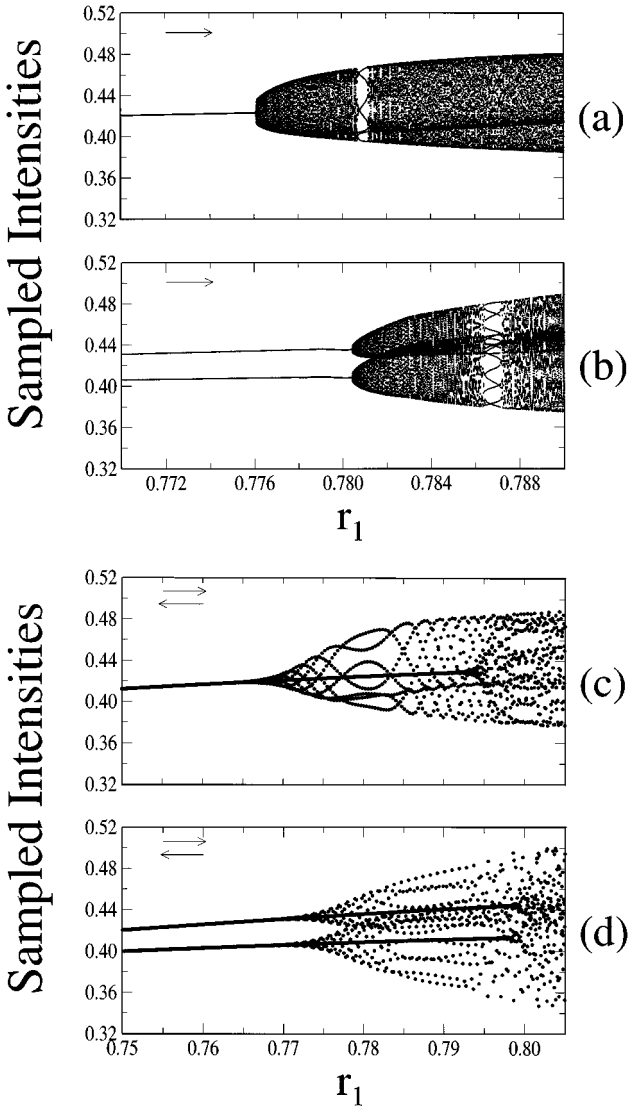

FIG. 6. Bifurcation diagram in the case of a transition to chaos via quasiperiodicity. (a) Reference diagram in the absence of subharmonic perturbation, (b) in the presence of in-phase ($\varphi=0$) subharmonic ($n=2$) modulation, (c) and (d) the same with a dynamic deformation of the bifurcation diagram induced by a nonadiabatic sweep rate.

perturbation. This is the case with $r_1 \cong 0.781$ and a subharmonic perturbation with $r_2=0.02$ and $\varphi=0$ transforms the unperturbed $7T$ periodic response into a quasiperiodic one [see Figs. 6(a) and 6(b)].

As will be seen in the experimental section, the direct recording of the bifurcation diagrams is made difficult by technical fluctuations. As a compromise between fluctuations and adiabatic sweeping conditions, we had to choose a sweep rate in which the bifurcation diagrams are only slightly deformed by the fast passage across the bifurcations. Numerical simulations have been carried out to check that the dynamical deformation of the bifurcation diagrams does not alter drastically the effects discussed here with sweep rates similar to those used in the experiments. Two sets of simulations have been carried out for two different sweep rates of the modulation index ($dr_1/d\tau=6.6\times10^{-10}$ and 2.2×10^{-12}) corresponding, respectively, to the standard experimental sweep rate of about 1 Hz and to a very slow rate ensuring good convergence toward the long-time limit but experimentally inaccessible. The slow sweep results are reported in Figs. 5(a) and 5(b), discussed above, and Figs. 6(c) and 6(d) show two bifurcation diagrams dynamically deformed by the nonadiabatic sweep. The abrupt jump in the sampled amplitudes that was observed at the bifurcation point in the quasistatic regime is smoothed in both the 6(c) and 6(d) diagrams and the shift of the bifurcation point induced by the sweep compounds that induced by the subharmonic additional modulation. The results obtained at a rate corresponding to experimentally accessible values exhibit a dynamical hysteresis shift of the bifurcation points and the associated dynamical hysteretic effects [18,19].

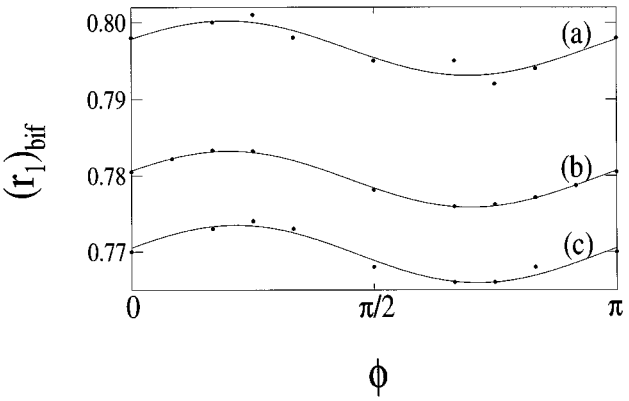

FIG. 7. Influence of the phase φ of subharmonic perturbation on the transition point from periodic to quasiperiodic response for two different sweep rates of the modulation index. The position of the bifurcation to quasiperiodicity is given for (a) increasing modulation amplitudes, (b) quasistatic conditions, (c) decreasing modulation amplitudes.

The nature and the amplitude of the effects are not modified when quasistatic conditions are used instead of nonadiabatic ones. This is validated by a quantitative comparison of the evolution of the bifurcation points with the dephasing φ. In Fig. 7 we have plotted the evolution of the position of the bifurcation to quasiperiodicity, i.e., the shift (i) discussed above versus the phase φ of the second modulation. Both dynamical and quasistatic results show the same sinusoidal dependence of the shift versus φ and all curves are just globally shifted by the dynamical (sweep) effect. Note that the quasistatic bifurcation point always shifts to larger modulation values as indicated by its position above the reference ($r_1=0.776$). Moreover, the shifts may be fitted by purely sinusoidal laws such as those indicated by the continuous curves shown in Fig. 7.

As already mentioned in the case of the period-doubling cascade, it is necessary to consider the whole bifurcation diagram to understand the change in the dynamics due to the second perturbation. For instance, a single phenomenon such as the shift of the bifurcation diagram may be used to change a chaotic regime into a periodic one and vice-versa, depending only on the operating conditions of the laser and on the phase of the perturbation. It is then clear how and why the phase of the subharmonic perturbation could be used both for control and for creating chaos.

VI. QUASIPERIODICITY—EXPERIMENTS

By adjusting the laser parameters and, more specifically, the pump parameter $A=2.5$ and the modulation frequency, which is now 12.75 kHz and corresponds approximately to $0.4\Omega_R$, it has been possible to observe a transition to quasiperiodicity in the laser with the main modulation only. In the first series of experiments, the laser is subjected to an additional $n=2$ subharmonic modulation. The amplitude of the additional modulation was set to 0.02 so as to keep it much smaller than the main modulation, which was swept between 0.35 and 0.7. This sweep amplitude is much larger than that used in the numerical simulations because technical noise induces large fluctuations, especially in the vicinity of the bifurcation points, and large sweeps are required to exhibit clearly the bifurcation diagrams. Using such large sweeps produces unavoidable dynamical distortions of these diagrams, as discussed in the preceding section. As for the numerical simulations, both forward and backward sweeps are superimposed on the display in order to exhibit the hysteresis phenomena and the dynamical deformations of the bifurcation diagrams.

The most striking effect observed experimentally is the enhancement of the dynamical shift of the bifurcation point and the associated change in the shape of the bifurcation diagram already discussed with respect to numerical results. This is clear here on the central part of the perturbed bifurcation diagram, where the full line associated with the periodic regime obtained for increasing values coincides with the spread values of the quasiperiodic regime that exists for a larger range at decreasing r_1 values.

The exploration of experimental bifurcation diagrams also revealed a new effect that was not obtained in the numerical simulations reported above, namely, the switching to a new attractor induced by the additional perturbation. This phenomenon appears clearly on the left-hand side of the diagram shown in Fig. 8, which was obtained for a first subharmonic modulation ($n=2$). At large modulation amplitudes, the laser switches from the quasiperiodic behavior to a $2T$ attractor that later destabilizes in a quasiperiodic attractor. These new attractors are significantly different from the original ones that appeared in the low- and medium-modulation domains. This phenomenon is made clearer because of the hysteresis effect that accompanies it, since, as the modulation amplitude is decreased, the laser remains on a $2T$ attractor in a wider range than for increasing amplitudes until it eventually switches back to the perturbed original attractor. This generalized bistability effect must be related to the sequential horseshoe formation already discussed in models of class-B lasers by Schwartz [20] and whose effect in the form of generalized bistability has been observed in CO_2 lasers since the early experiments on chaos in these lasers [19,21]. Since doped fiber lasers such as the one used in the present experiments belong to the same class of lasers, it may be anticipated that they should present the same phenomenology.

In this section, we present some results in the form of local results, i.e., results obtained for a given set of parameters and not as full bifurcation diagrams, because here the former are more suitable for exhibiting unambiguously some qualitative changes in the dynamical regimes. The basic change is illustrated in Fig. 9 where time traces of the laser

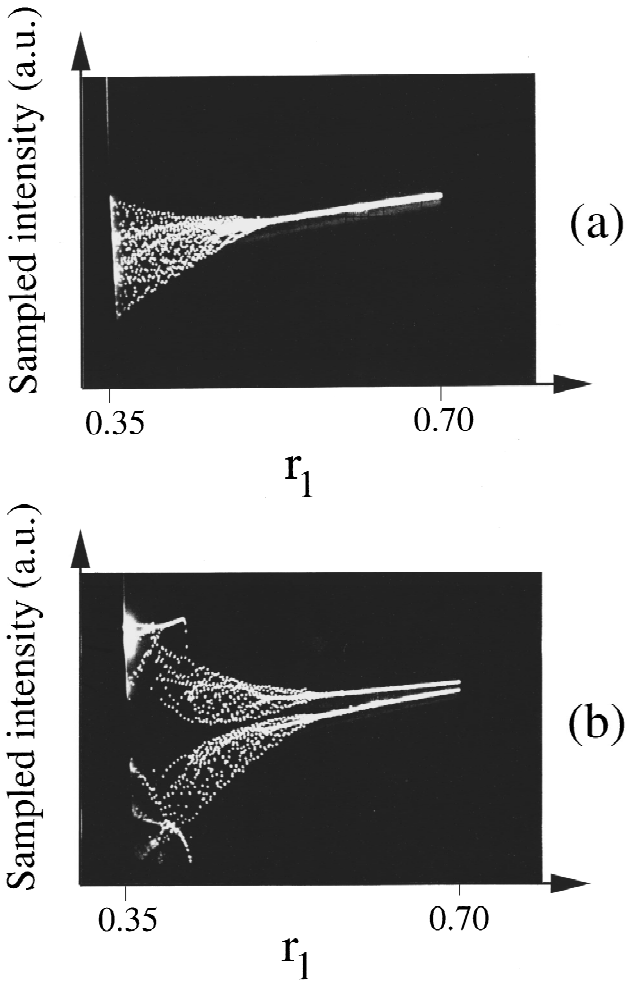

FIG. 8. Experimental observations of bifurcation diagrams of the fiber laser in the case of the transition to quasiperiodicity (a) in the absence and (b) in the presence of $n=2$ subharmonic modulation with phase $\varphi=13\pi/9$. The amplitude of the driving field is swept between 0.35 and 0.7 at a rate of 1 Hz.

output are displayed (a) in the absence and (b) in the presence of the second perturbation. With the main trace, the laser intensity varies quasiperiodically with time, while the presence of a fourth subharmonic perturbation at 3.1875 kHz and phase $\varphi=3\pi/2$ changes the original quasiperiodic behavior into an $8T$ periodic one.

The periodicity of the signal in the presence of the subharmonic perturbation which is already clear in the time trace is confirmed by examination of the first-return maps shown in Fig. 10. Such a map is obtained by plotting a sampled value obtained by periodic sampling versus the value sampled at the preceding period, which is kept in a temporary buffer memory. Through such a technique, it has been possible to obtain first-return maps in real time on an oscilloscope. As mentioned above, a series of discrete points corresponds to a periodic regime, while a closed curve is the signature of quasiperiodicity. With the experimental parameters chosen here, this first-return map is equivalent to a Poincaré section. This section is achieved in a plane of constant phase of the main modulation, i.e., $\Omega\tau=\text{const}(\text{mod}2\pi)$ in the cylindrical phase space $[x(t),\Omega\tau,x(t+T)]$. For a three-dimensional phase space,

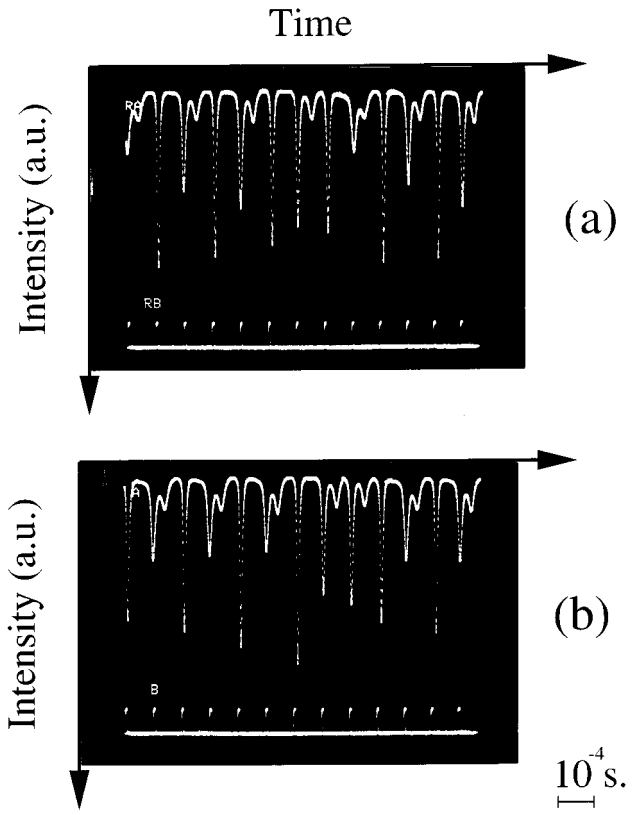

FIG. 9. Experimental observation of phase control in the case of a quasiperiodic regime. Temporal evolution of the laser output intensity (a) quasiperiodic regime in the presence of the driving only, (b) period-8 response when a weak $n=4$ subharmonic modulation is added ($r_1=0.438$ and $r_2=0.02$).

both Poincaré section and first return map are equivalent under these conditions.

The Poincaré section obtained in the absence of subharmonic modulation [Fig. 10(a)] consists of two symmetric closed curves and are typical of a quasiperiodic regime. We have explored here the situation of $n=2$ subharmonic modulation with an amplitude of 0.02 while the main driving amplitude is 0.438. Two return maps corresponding to phases $\varphi=0$ and $\pi/18$ show that, depending on φ, this perturbation may have the opposite effects. The former drives the system towards a period-8 response [Fig. 10(b)] while the latter leads it to a chaotic regime [Fig. 10(c)]. Note that here control of the dynamics through the phase of the subharmonic perturbation is very efficient and versatile, since it has also been possible to set very different dynamical regimes (periodic, quasiperiodic, and chaotic) just by choosing a different phase for the controlling perturbation.

The reverse control situation is illustrated in the diagrams presented in Fig. 11, now with fourth subharmonic modulation. More precisely, the unperturbed system is chaotic and the perturbed one may become periodic or stay chaotic, depending on the phase of the second perturbation, as illustrated by the different Poincaré sections shown in Fig. 11. The reference diagram obtained in the absence of the second perturbation [Fig. 11(a)] is typical of a chaotic regime. An adequate choice of the phase of the second perturbation, e.g., $\varphi=29\pi/18$ allows one to drive the system into periodic regimes [see Fig. 11(d)] while a perturbation with the same

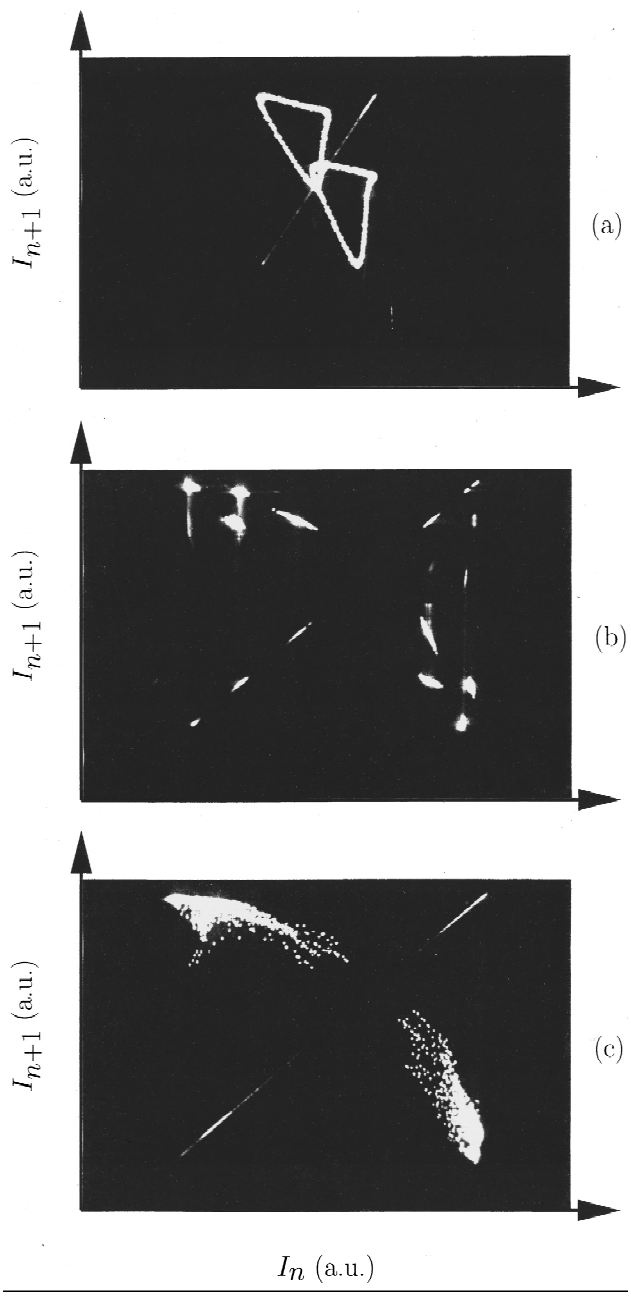

FIG. 10. Experimental observation of phase control from a quasiperiodic state in the case of an $n=2$ subharmonic perturbation. (a) Reference quasiperiodic state, (b) $\varphi=0$ period-8 regime, (c) $\varphi=\pi/18$ perturbed chaotic state. $r_1=0.438$ and $r_2=0.02$.

amplitude and a phase of π would leave it in the chaotic domain [see Fig. 11(b)]. Note that with $\varphi=10\pi/9$ [Fig. 11(c)] the dynamics are qualitatively changed. The system is no longer in the fully chaotic regime but rather in the C8 region of the inverse cascade, which occurs at the beginning of the chaotic domain.

VII. CONCLUSIONS

Both experimental investigations and numerical simulations show that the phase of a subharmonic modulation plays a major role in controlling the dynamics of a driven system. To understand even qualitatively the nature of this effect, it

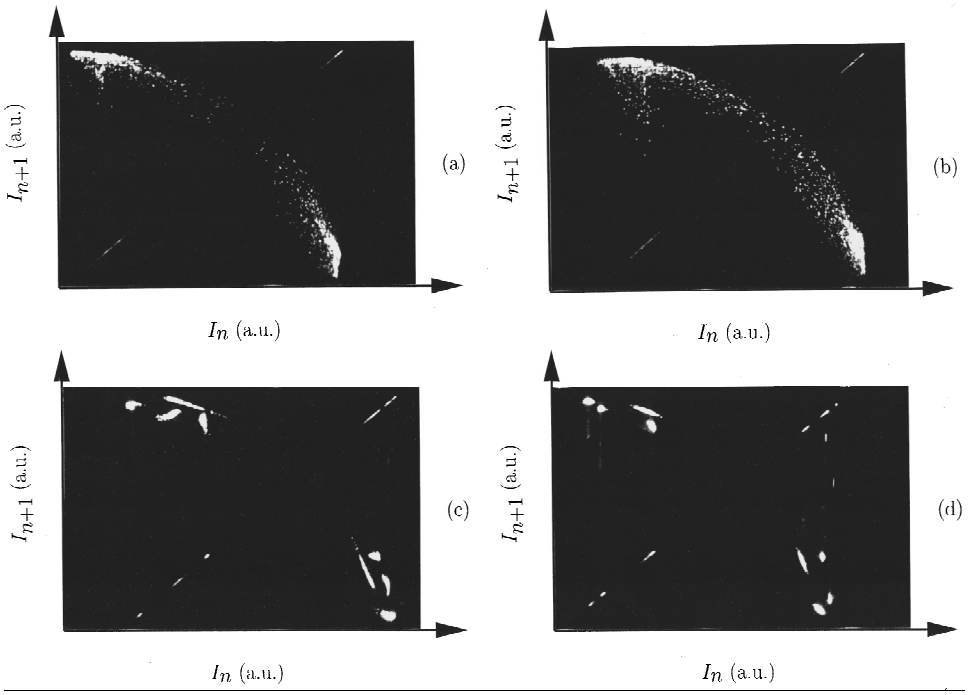

FIG. 11. Experimental observation of phase control from a chaotic state obtained through quasiperiodicity in the case of an $n=4$ subharmonic perturbation (main driving frequency 12.75 kHz, $r_1=0.438$ and $r_2=0.02$). Evolution of the Poincaré sections. (a) Chaotic regime in the presence of the driving only, (b) with added $n=4$ subharmonic perturbation at $\varphi=\pi$. The response is chaotic (c) $\varphi=10\pi/9$ chaotic-8 response and (d) $\varphi=29\pi/18$ 8T periodic response $r_1=0.438$ and $r_2=0.02$.

is necessary to consider globally the bifurcation diagrams. This has allowed us to give a more accurate view of the effects of such small subharmonic perturbations on various dynamical regimes including quasiperiodicity and chaos of a nonlinear system. Major changes of the bifurcation diagram have been observed such as shifts of bifurcations, crises, and new attractors. By considering the bifurcation diagram globally, we discovered how different regimes emerge or disappear as the amplitude of second modulation is progressively increased. Based on the knowledge gained from these bifurcation diagrams, it has been possible to switch from chaotic to quasiperiodic or periodic regimes and vice versa, depending on both the operating conditions and the perturbation parameters. The approach presented here provides us with a unitary point of view on several experiments dealing with the control of dynamical regimes by subharmonic perturbations resulting in a global simplification of the results. It showed that the possibility of controlling the dynamics through the phase of a subharmonic perturbation is quite general. It holds for both the period-doubling cascade and the quasiperiodic route to chaos and has been checked for both second and fourth subharmonics.

Simulations and experiments reported here are only a small part of the field open by the use of subharmonic modulation. However the variety of the dynamical changes observed indicate that it should be possible to ''tailor'' a subharmonic perturbation to reach the specific regime. It may be anticipated that other subharmonic ratios should also actively control chaos but with efficiencies that should depend not only on the selected subharmonic ratio but also on the parameters that determine the chaotic regime, since the nature and the stability of unstable periodic orbits should play a major role in the possibilities of controlling chaos.

ACKNOWLEDGMENTS

The authors wish to thank the Région Nord–Pas de Calais and the FEDER for funding. S. Bielawski and D. Derozier are acknowledged for their help and for discussions on the model. T. Newell, A. Gavrielides, V. Kovanis, T. Erneux, and D. Sukow kindly communicated to us their results prior to publication. The Laboratoire de Spectroscopie Hertzienne is Equipe Associée au CNRS (URA 249) and a member of the Center d'Etudes et de Recherches sur les Lasers et leurs Applications (CERLA).

[1] E. Ott, C. Grebogi, and J. A. Yorke, Phys. Rev. Lett. **64**, 1196 (1990).
[2] R. Lima and M. Pettini, Phys. Rev. A **41**, 726 (1990).
[3] P. Bryant and K. Wiesenfeld, Phys. Rev. A **33**, 2525 (1986).
[4] M. Ciofini, R. Meucci, and F. T. Arecchi, Phys. Rev. E **52**, 94 (1995).
[5] Y. Liu and J. R. Rios Leite, Phys. Lett. A **185**, 35 (1994).
[6] N. Watanabe and K. Karaki, Opt. Lett. **20**, 1032 (1995).
[7] R. Corbalan, J. Cortit, A. N. Pisarchik, V. N. Chizhevsky, and R. Vilaseca, Phys. Rev. A **51**, 663 (1995).
[8] P. Glorieux, C. Lepers, R. Corbalan, J. Cortit, and A. N. Pisarchik, Opt. Commun. **1118**, 309 (1995).
[9] R. Meucci, W. Gadomski, M. Ciofini, and F. T. Arecchi, Phys. Rev. E **49**, R2528 (1994).
[10] J. Yang, Z. Qu, and G. Hu, Phys. Rev. E **53**, 4402 (1996).
[11] T. Newell, A. Gavrielides, V. Kovanis, T. Erneux, and D. Sukow (private communication).
[12] Z. Qu, G. Hu, G. Yang, and G. Qin, Phys. Rev. Lett. **74**, 1736 (1995).
[13] S. T. Vohra, L. Fabiny, and F. Bucholtz, Phys. Rev. Lett. **75**,

65 (1995).
[14] S. Bielawski, D. Derozier, and P. Glorieux, Phys. Rev. A **46**, 2811 (1992).
[15] Ya. I. Khanin, *Principles of Laser Dynamics* (North-Holland, Amsterdam, 1995).
[16] B. B. Flapp and A. W. Hübler, Phys. Rev. Lett. **65**, 2302 (1990).
[17] V. N. Chizhevsky and S. I. Turovets, Phys. Rev. A **50**, 1840 (1994).
[18] P. Mandel and T. Erneux, Phys. Rev. Lett. **53**, 1818 (1984); P. Mandel, in *Frontiers in Quantum Optics*, edited by E. Pike and S. Sarkar (Adam Hilger, Bristol, 1986).
[19] D. Dangoisse, P. Glorieux, and D. Hennequin, Phys. Rev. A **36**, 4775 (1987).
[20] I. B. Schwartz, Phys. Rev. Lett. **60**, 1359 (1988); Phys. Lett. A **126**, 411 (1988).
[21] J. R. Tredicce, F. T. Arecchi, G. P. Puccioni, A. Poggi, and W. Gadomski, Phys. Rev. A **34**, 2073 (1986); H. G. Solari, E. Eschenazi, R. Gilmore, and J. R. Tredicce, Opt. Commun. **64**, 49 (1987).